Uchimura et al., http://www.jcb.org/cgi/content/full/jcb.201407039/DC1

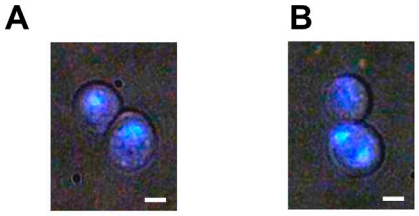

C

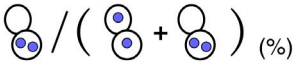

(%)

WT	2
Δ*dyn1*	20

α-Tubulin		β-Tubulin	
E387A	1	E376A	0
E390A	0	K379A	3
R391A	0	D383A	2
R394A	0	K390A	0
K395A	5	R391A	0
K402A	2	K392A	3
E412A	0	E401A	0
R423A	1	D404A	1
E424A	4	E405A	0
D425A	4	E412A	1
E430A	1		
R431A	4		
D432A	3		
E435A	1		

Figure S1. **Nuclear distribution at anaphase in yeast tubulin mutants.** DAPI fluorescence image showing the position of the nuclei was merged with a phase-contrast image for wild-type (A) and Δ*dyn1* mutant (B) cells. The latter show a typical binucleation phenotype. (C) Percentage of binucleated cells. In total, 100 cells were counted for the wild type, Δ*dyn1*, and each tubulin mutant. Bars, 2 µm.

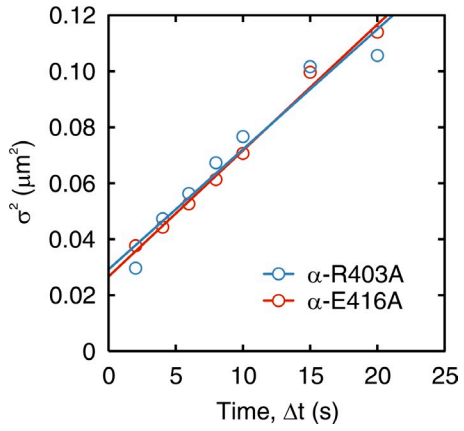

Figure S2. **Diffusional property of MTs interacting with multiple dynein molecules in the MT-gliding assay.** The distribution of the displacement (Δ*x*) in a particular time period (Δ*t*) was fitted by the sum of two Gaussian distributions corresponding to stationary phase and diffusional phase (Fig. 2 B). The variance (σ^2) of the distribution for the diffusional phase was plotted against Δ*t*, and the diffusion coefficient (*D*) was obtained from the slope of the line by the equation $\sigma^2 = 2D\Delta t + 2\delta^2$, where δ represents tracking precision. The values were $D = 0.0021$ µm^2/s and $\delta = 0.12$ µm for α-R403A and $D = 0.0022$ µm^2/s and $\delta = 0.12$ µm for α-E416A.

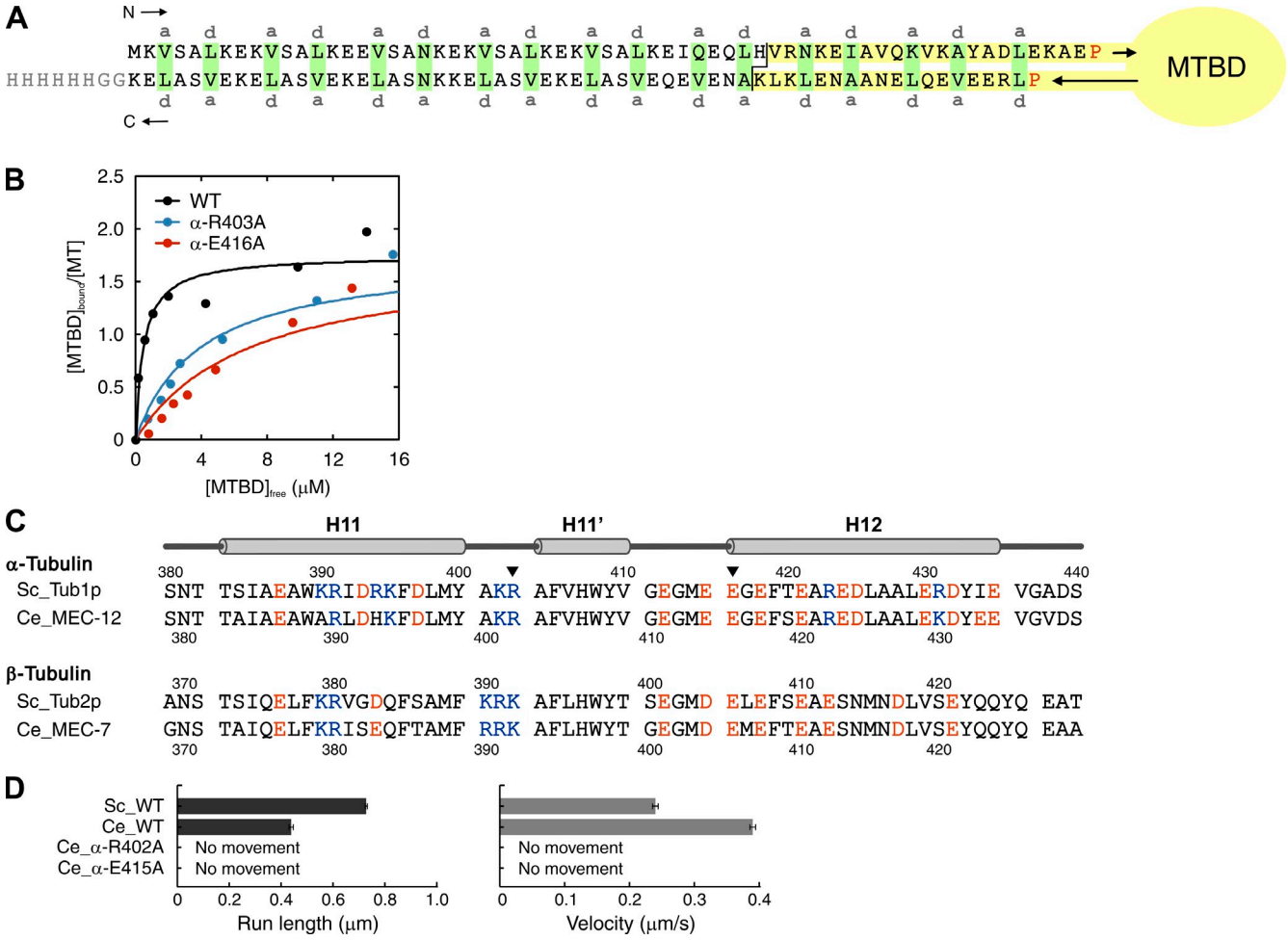

Figure S3. **Characterization of MTBD and 15-pf MT used in cryoEM analysis.** (A) Design of MTBD construct fixed in α registry. The sequence derived from the distal end of the slime mold dynein stalk (V3350-K3514, highlighted in yellow) is fused to the artificial coiled coil at a site indicated by the black line. Conserved proline residues P3371 and P3496 in the stalk coiled coil and a His6 tag (with GG linker) at the C-terminal end of the construct are red and gray, respectively. When fixed in this registration, the dynein motor domain is trapped in a state with high ATPase activity and strong MT-binding affinity (Gibbons et al., 2005; Kon et al., 2009). (B) Binding of the dynein MTBD to wild-type, α-R403A, and α-E416A yeast MTs. A cosedimentation assay was conducted in PK buffer at a MT concentration of 2 μM. The graph shows a typical example out of two independent sets of measurements. For wild-type MTs, the dissociation constant and the stoichiometry of binding, obtained by fitting a hyperbola, were 0.6 μM ± 0.1 and 1.5 ± 0.3, respectively (mean ± SEM). For mutants, binding was not saturated in the concentration ranges measured. Assuming that the binding stoichiometry for wild type and mutants is the same, the dissociation constant was calculated to be 6.2 ± 2.1 and 10.8 ± 3.8 μM for α-R403A and α-E416A, respectively. (C) Sequence alignment of tubulins from yeast *S. cerevisiae* (Sc) and nematode *C. elegans* (Ce). Positively and negatively charged residues are blue and red, respectively. The positions of R403 and E416 of α-tubulin are indicated by an arrowhead. (D) Results of the single-molecule motility assay with a 15-pf MT composed of nematode tubulin. Two-headed dynein did not move on MTs with mutations of α-R402A and α-E415A, which is equivalent to α-R403A and α-E416A in yeast tubulin.

A

Number of micrographs	1,407
Number of filaments	3,809
Total number of segmented images in initial selection	99,128
Total number of segmented images used in final map	98,487
The number of asymmetric units	1,477,305
Resolution (FSC† = 0.143)	8.2 Å
Resolution (FSC† = 0.5)	9.3 Å

†Fourier shell correlation

B

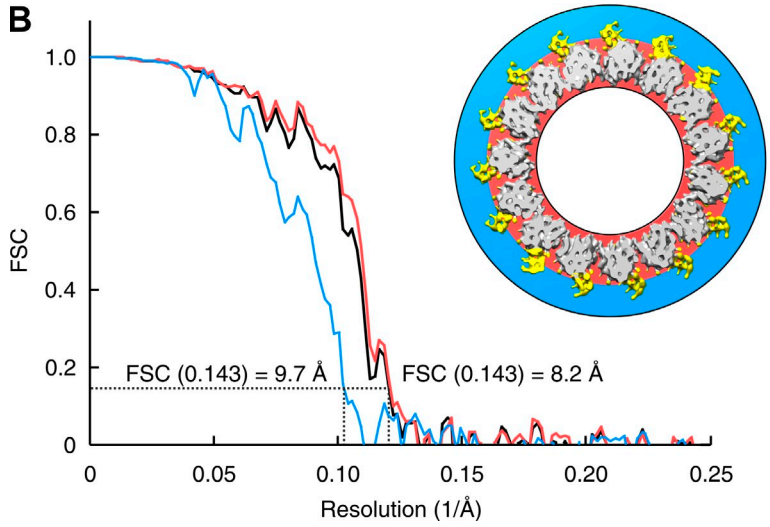

Figure S4. **Image processing statistics and resolution of the cryoEM map.** (A) Summary of image-processing statistics. (B) Evaluation of the resolution of the cryoEM map. The images used for the final map were randomly split in half, 3D image reconstruction was performed independently for each dataset, and Fourier shell correlation (FSC) curves were computed for these two independent reconstructions. The resolution of the complete volume, estimated by using the FSC = 0.143 criterion, is 8.2 Å (black line). This value is the same as that for the volume composed mostly of MTs (red in the map), for which the correlation curve is shown in red, but higher than the 9.7-Å resolution of the volume containing only the MTBD (blue in the map), for which the correlation curve is shown in blue.

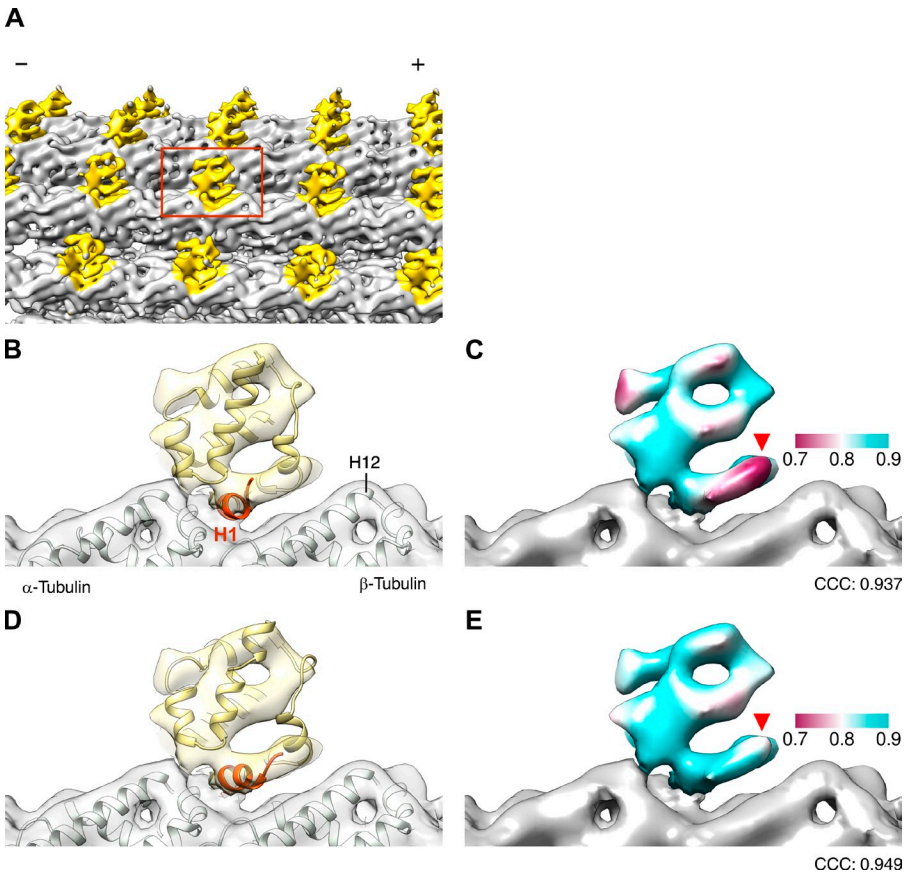

Figure S5. **Model building and assessment.** (A) Outside view of the 8.2-Å resolution map of the MTBD–MT complex. The MT is colored gray and the MTBD in yellow. The MT polarity is indicated. The single MTBD density boxed in red was used for assessment of models (B–E). To build a pseudo-atomic model of MTBD bound to MT, the MTBD structure (T3382-E3489) derived from slime mold dynein (PDB ID: 3VKH; Kon et al., 2012) was fitted into the cryoEM map as a rigid body (B) and then refined by flexible fitting with the DireX and Flex-EM program (D; Topf et al., 2008; Wang and Schröder, 2012). The quality of each model was assessed by calculating the cross-correlation coefficient (CCC) between the experimental and the simulated map at a resolution of 9 Å (C and E, respectively). The tube density, marked by red arrowheads in C and E, was not filled by the model in the rigid-body fitting (B), but was occupied by helix H1 and its N-terminal loop in the model refined by flexible fitting (D), as clearly indicated by the difference in the cross-correlation coefficient, which was colored purple for low to blue for high cross-correlation coefficient (C and E).

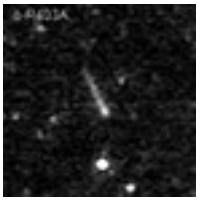

Video 1. **Motion of wild-type, α-R403A, and α-E416A MTs in the MT-gliding assay.** The behaviors of wild-type and mutant MTs on a dynein-coated glass surface in the presence of ATP were observed under a dark-field microscope (BX50; Olympus). The bright segment of each MT represents a fluorescently labeled seed for polymerization, located near the minus end of the MT. Bar, 2 µm. This movie is related to Fig. 2.

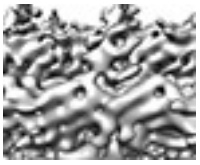

Video 2. **Flexible fitting of MTBD crystal structure into the cryoEM map of the MTBD–MT complex.** The crystal structure of the MTBD (T3382-E3489) derived from slime mold dynein (PDB ID: 3VKH) was used for fitting. Morphing between the two models built by rigid body and flexible fitting was calculated using the Morph Conformations tool in UCSF Chimera and recorded as a movie. This movie is related to Figs. 4 and S5.

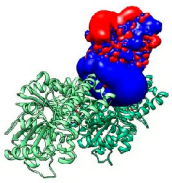

Video 3. **A profile of the isopotential contour for MTBD bound on MT.** The electrostatic potential of the MTBD structure generated in this study (Fig. 4) was calculated using an Adaptive Poisson-Boltzmann Solver (Unni et al., 2011). The contours at −2.5 kT/e (red) and 2.5 kT/e (blue) are shown. This movie is related to Fig. 5 C.

References

Gibbons, I.R., J.E. Garbarino, C.E. Tan, S.L. Reck-Peterson, R.D. Vale, and A.P. Carter. 2005. The affinity of the dynein microtubule-binding domain is modulated by the conformation of its coiled-coil stalk. *J. Biol. Chem.* 280:23960–23965. http://dx.doi.org/10.1074/jbc.M501636200

Kon, T., K. Imamula, A.J. Roberts, R. Ohkura, P.J. Knight, I.R. Gibbons, S.A. Burgess, and K. Sutoh. 2009. Helix sliding in the stalk coiled coil of dynein couples ATPase and microtubule binding. *Nat. Struct. Mol. Biol.* 16:325–333. http://dx.doi.org/10.1038/nsmb.1555

Kon, T., T. Oyama, R. Shimo-Kon, K. Imamula, T. Shima, K. Sutoh, and G. Kurisu. 2012. The 2.8 Å crystal structure of the dynein motor domain. *Nature*. 484:345–350. http://dx.doi.org/10.1038/nature10955

Topf, M., K. Lasker, B. Webb, H. Wolfson, W. Chiu, and A. Sali. 2008. Protein structure fitting and refinement guided by cryo-EM density. *Structure*. 16:295–307. http://dx.doi.org/10.1016/j.str.2007.11.016

Unni, S., Y. Huang, R.M. Hanson, M. Tobias, S. Krishnan, W.W. Li, J.E. Nielsen, and N.A. Baker. 2011. Web servers and services for electrostatics calculations with APBS and PDB2PQR. *J. Comput. Chem.* 32:1488–1491. http://dx.doi.org/10.1002/jcc.21720

Wang, Z., and G.F. Schröder. 2012. Real-space refinement with DireX: from global fitting to side-chain improvements. *Biopolymers*. 97:687–697. http://dx.doi.org/10.1002/bip.22046

A ZIP file provides an R script to analyze a kymograph of the MT movements.